From a compressible fluyid model to new mass conserving cavitation algorithms

Guy Bayada

June 6 2013

From a compressible fluid model to New mass conserving cavitation algorithms

G. BAYADA

Institut Camille Jordan ,UMR CNRS 5208, Université de Lyon

Mathématiques -INSA de Lyon

F 69621 Villeurbanne Cedex

Tel 33472438312 Fax 33472438529

guy.bayada@insa-lyon.fr

Jakobson.Floberg.Olsson /Elrod.Adams mass conserving cavitation model is very popular , however numerically difficult to manage.

The main idea of this paper is that the J.F.O./E.A. model can be viewed as a compressible Reynolds equation with a specific density-pressure law. Approximation of this pressure - density law originating from a 3-dimensional model of vaporous cavitation has been proposed. This physically justified approximation covers the wide range of the pressure including the liquid-vapor transition. New mass conserving algorithms are proposed . One of them is implicit. Main advantage of this implicit algorithm is that it can be implemented very easily: exactly as the well known Christopherson algorithm. Moreover it can be extended to unsteady cavitation problems without difficulties. Various numerical examples are given to show the stability of this kind of approximation as well as the great diminution of time computation by using some over relaxation parameter.

Abstract:

This study investigates two algorithms proposed to solve a new cavitation model. This new cavitation model is based on a compressible Reynolds equation in which the density-pressure

relation is obtained from a barotropic-isentropic assumption. It can be viewed as an approximation of the Jakobson-Floberg-Olsson /Elrod Adams cavitation model. Two algorithms are proposed to solve it. The first one is explicit and needs a important number of nodes. The second is implicit and can be used for steady-state and unsteady problems. Its implementation is easy and needs only minor modifications for a computer code in which cavitation is ignored. It can also be used to compute the solution of the usual J.F.O./E.A. model. Faster convergence is obtain using a relaxation parameter.

Keywords: hydrodynamic lubrication; Compressible Reynolds equation; Cavitation algorithm

Highlights :

- A new cavitation model as an approximation of usual Jakobsson-Floberg-Olsson/Elrod-Adams model
- New implicit Cavitation algorithm proposed for both J.F.O./E.A. and this new model

- Algorithm easily implemented for finite difference and finite element discretization
- Algorithm available for both steady state and unsteady problems
- Acceleration of the convergence with an over-relaxation parameter

1 Introduction

Cavitation in lubrication is a complex process which has been the subject of numerous studies , both from the physical aspect and the numerical one[1]. The boundary conditions used to describe the

cavitation region are usually a zero pressure gradient and a constant given value p_{cav} (the so called cavitation pressure). This constant value is often assumed on the whole cavitation area while the sign restriction $p>p_{cav}$ is applied on the non cavitated area. This model has often been called the Reynolds cavitation model. For a long time, Christopherson algorithm [2]has been widely used to described the cavitation. One of its primary quality is it is easy to perform : It is a slight modification of the well-known Jacobi or Gauss Seidel algorithms used to solve the system of equations obtained by discretizing Reynolds equation using finite elements or finite difference methods: The only modification being the introduction of an additional line which modifies each computed term which is less than p_{cav} and puts it to this value during the iterative procedure. The main disadvantage of this model is that it is not a mass-conserving one. This feature can often be neglected in a lot of situations (plain journal bearing or slider in fully flooded situation) if the load or the attitude angle are the only operational parameters of interest. However if input mass flow values have to be considered, if starvation occurs or if roughness cannot be neglected, the Reynolds cavitation model must not be used [18]. Most of the works about mass conserving cavitation models are based on the Jakobsson-Floberg-Ollson (J.F.O.)[3]cavitation model and the Elrod Adams (E.A.)algorithm[4]. The basic idea is to describe the mass flow not only as a function of the pressure p but also of an another unknown θ which is the relative saturation (or fluid saturation) with the constraints

$$p \geq p_{cav},\ 0 \leq \theta \leq 1,\ (p - p_{cav})(\theta - 1) = 0 \qquad (1)$$

The model is a conservative one by construction. it is however mathematically much more complicated : hyperbolic in the cavitation area and elliptic in the non cavitated area .

The present proposed paper will address three aspects of the previous mentioned cavitation J.F.O/E.A.models:

-It is difficult to obtain them in a rigorous way using a thin film procedure, starting from a full 3 dimensional description . For example the E.A. model is obtained by a modification of a mass flow description which is only valid assuming a homogeneous 3-dimensional flow [4]

-All these models assume the fact the pressure never falls below the cavitation pressure p_{cav}. However sub-ambient pressure loops have been observed as early as 1982 by Etsion and Ludwig[5] and Braun and Hendricks[6] one year later. Values of pressure as small as 0.07MPA have been observed. The existence of such under-pressure can be neglected for heavily loaded devices. For light loaded devices however, the constraint $p>p_{cav}$ cannot be retained and previous models are not suitable. Moreover, fluid properties (viscosity, density) inside the cavitation area cannot be taken into account.

-Although it is possible to prove that the J.F.O./E.A model is a well posed problem [7], the computation of the solution is not easy. Elrod and Adams identify as a difficulty the fact that the relation θ-p in equation (1) is not one to one (for example the value θ=1 is not associated to a unique value of the pressure). They modify this relation in the non cavitated area by introducing a small compressibility parameter. Numerous methods have been proposed to deal with both E.A and J.FO. models. Most of them are based on the E.A algorithm and its Vijayaraghvan –Keith improvement [8] by introducing various iterative process coupling pressure and saturation [9][10]. Some others used the characteristic methods to deal with the hyperbolic feature of the equation [11]. In some particular cases it is possible to consider a system of coupled ordinary differential equations instead of the partial differential equation [12]. Recently the Linear Complementarity numerical method has been used to solve the discretized problem [13]. All these methods are not easy to implement, so that, despite their physical disturbing feature, Christopherson method is often used even today.

Recently, a thin film procedure starting from the compressible3-dimensional Navier-Stokes equation with variable density and (dynamic) viscosity has been rigorously performed [14]. Assuming

simplified properties (barotropic and isentropic assumptions)of the fluid ,a Reynolds compressible equation is obtained which is very close to the E.A. model and improved it in some aspects:

-No geometrical assumption about the shape of the cavitation area

-Variation of both density and viscosity in cavitation region and in "full film" region can be considered

-No constraint like $p>p_{cav}$ is introduced so that under-pressure can be obtained.

Detailed properties of this new model which will be called 'fully compressible model"(FC) have been already given [15]. We discuss in this paper numerical algorithms to solve this model. We will show how a simplified numerical mass conserving algorithm can be deduced for the JFO-EA model. This algorithm is very close to the well-known Christopherson algorithm and so is very easy to implement.

2 New "fully compressible" fluid model

The Reynolds equation is written for a model device with a small gap $h(x_1,x_2)$ in which the upper part is fixed and the flat lower part has a constant velocity u along the x_1-main direction. Neglecting variation of the temperature, viscosity μ and density ρ are assumed to be only function of the pressure.

$$\frac{\partial}{\partial x_1}\left(\frac{h^3}{12\mu(\rho)}\rho(p)\frac{\partial p}{\partial x_1}\right)+\frac{\partial}{\partial x_2}\left(\frac{h^3}{12\mu(\rho)}\rho(p)\frac{\partial p}{\partial x_2}\right)=u/2\frac{\partial(\rho(p)h)}{\partial x_1}+\frac{\partial(\rho(p)h)}{\partial t} \qquad (2)$$

Although this equation is written for transient situations, it will firstly be considered for a steady state situation, so neglecting the time derivative term. Dynamic aspects will be treated in section 5 .

The cavitation phenomenon is implicitly contained in the density-pressure relation in the context of the vaporous cavitation. Three distinct regimes are considered: one of pure vapour,

one for pure liquid and one of mixture. The input data are: the velocities of the sound, c_v and c_l , the density ρ_v and ρ_l and the viscosities μ_v and μ_l in each of the pure regimes. From these data, it is possible to compute the transition pressure between these 3 regimes: p_{vm} between vapour and mixture and p_{sat} between mixture and liquid:

$$p_{vm} = \rho_v c_v^2 \qquad (3a)$$

$$p_{sat} = \rho_v c_v^2 - N \log\left(\frac{\rho_v^2 c_v^2}{\rho_l^2 c_l^2}\right) \qquad (3b)$$

$$\text{with } N = \frac{\rho_v c_v^2 \rho_l c_l^2 (\rho_v - \rho_l)}{\rho_v^2 c_v^2 - \rho_l^2 c_l^2} \qquad (3c)$$

It is convenient to introduce the void fraction α defined by:

$$\alpha = (\rho - \rho_{l)} / (\rho_v - \rho_l)$$

Pressure-density relations are:

$$p(\alpha) = c_v^2 \rho \qquad if\ \rho < \rho_v \qquad (4a)$$

$$p(\alpha) = P_{sat} + c_l^2 (\rho - \rho_l) \qquad if\ \rho > \rho_l \qquad (4b)$$

$$p(\alpha) = P_{sat} + N \log\left(\frac{\rho_v c_v^2 \rho}{\rho_l(\rho_v c_v^2 (1-\alpha) + \rho_l c_l^2 \alpha)}\right) \quad if\ \rho_v < \rho < \rho_l \qquad (4c)$$

In the mixture region, viscosity-density relation can be chosen as:

$$\mu(\alpha) = \alpha\mu_v + (1-\alpha)\mu_l \quad Dukler\ assumption \qquad (5)$$

or

$$1/\mu(\alpha) = M(\alpha)/\mu_v + (1 - M(\alpha))/\mu_l \quad McAdams\ assumption \qquad (6)$$

In which M is the mass volume fraction of the vapour defined for $0<\alpha<1$ by:

$$M(\alpha)=\alpha\frac{\rho_v}{\rho(\alpha)} \qquad (7)$$

A comparison of the present "full compressible" law with the one issued from the E.A./JFO model is given in figure (1). It is clear that the graph of the present law can be very close to the one of J.F.O./E.A. and so are also the pressures. This is especially true if the value p_{cav} used in the J.F.O./E.A model is chosen close to p_{sat} . In other words; the new model can be viewed as an approximation of the J.F.O./E.A model. This assertion will be numerically studied in the following section 4.

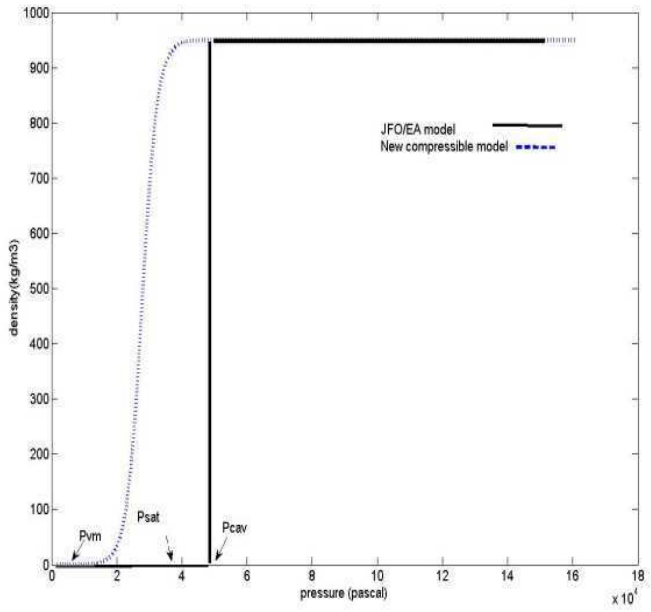

Figure1 : Pressure-density curves : A comparison of a fully compressible model and the J.F.O./E.A. model

3 Numerical algorithms for steady-state problems

We will describe two algorithms, one is a fully explicit method and the second is a half implicit one. The second algorithm prevents oscillations and needs less discretization'nodes . At last it is explained how it can be used to solve J.F.O./E.A model.

3.1 Fully explicit method

The solution is obtained (the index m tends to infinity) as the limit of the solutions (p^m) of a sequence of linear problem :

$$\frac{\partial}{\partial x_1}\left(\frac{h^3}{12\mu(p^{m-1})}\rho(p^{m-1})\frac{\partial p^m}{\partial x_1}\right)+\frac{\partial}{\partial x_2}\left(\frac{h^3}{12\mu(p^{m-1})}\rho(p^{m-1})\frac{\partial p^m}{\partial x_2}\right)=u/2\frac{\partial(\rho(p^{m-1})h)}{\partial x_1} \quad (8)$$

The first step is to perform a finite-difference or finite-element discretization of the Reynolds equation. Let us denote by Δx_1 and Δx_2 the discretization step in the x_1 and x_2 directions. Let p_k and ρ_k be the unknowns for the node M_k . Each linear problem is solution of a system of equations which can be written :

$$AP^m=B \quad (9)$$

In which P^m is the unknown vector .

Each term of the matrix A and of the right hand side term B are function of the values of pressure and density at the previous iterate.

Note that the finite difference discretization of the right hand side of(8)could be of various types:

Let (i Δx_1, jΔx_2) the coordinates of a node M_k, ((i +1)Δx_1, jΔx_2)those of M_K^+ and ((i-1) Δx_1, jΔx_2) those of M_k^- . We could then use:

$$\frac{\partial(\rho(p)h)}{\partial x_1}(M_k) \approx \frac{(\rho(p)h)(M_k) - (\rho(p)h)(M_k^-)}{\Delta x_1} \qquad (10a)$$

$$\frac{\partial(\rho(p)h)}{\partial x_1}(M_k) \approx \frac{(\rho(p)h)(M_k^+) - (\rho(p)h)(M_k)}{\Delta x_1} \qquad (10b)$$

$$\frac{\partial(\rho(p)h)}{\partial x_1}(M_k) \approx \frac{(\rho(p)h)(M_k^+) - (\rho(p)h)(M_k^-)}{2\Delta x_1} \qquad (10c)$$

Numerical experiments show that (10b) must be used to improve stability in this explicit schema.

3.2 (half)implicit method

The Reynolds compressible equation contains a great number of nonlinear terms . In terms of mathematical difficulty, there is however a great difference for the coefficients in the left hand side and in the right hand side: only the last ones control the mathematical nature of the equation (from elliptic to hyperbolic). The first terms can be treated by an explicit procedure without any problem of convergence. The proposed (half) implicit new procedure is based upon the solution of the sequence of nonlinear problems:

$$\frac{\partial}{\partial x_1}\left(\frac{h^3}{12\mu(p^{m-1})}\rho(p^{m-1})\frac{\partial p^m}{\partial x_1}\right)+\frac{\partial}{\partial x_2}\left(\frac{h^3}{12\mu(p^{m-1})}\rho(p^{m-1})\frac{\partial p^m}{\partial x_2}\right)=u/2\frac{\partial(\rho(p^m)h)}{\partial x_1} \quad (11)$$

After discretization, using formulae (10a) to treat the right hand side, we have to solve a system like :

$$AP^m=B\rho(P^m)+C \qquad (12)$$

In which all coefficients of A, B, C are known from the previous iterate:

Let us detail the k^{th} row of the system (12) for a given m:

$$p_k^m = 1/a_{k,k}\left(-\sum_{k\neq l} a_{k,l}\,p_l^m + \sum_{k\neq l} b_{k,l}\rho(p_l^m) + c_k + b_{k,k}\rho(p_k^m)\right) \qquad (13)$$

When using a Gauss Seidel procedure to solve (12), each component p_k^m is successively computed from the values of the pressure already known either from step m or step m-1.

$$p_k^m = 1/a_{k,k}(-\sum_{k\prec l} a_{k,l}\, p_l^m + \sum_{k\prec l} b_{k,l}\rho(p_l^m) + c_k + b_{k,k}\rho(p_k^m) - \sum_{k\succ l} a_{k,l}\, p_l^{m-1} + \sum_{k\neq l} b_{k,l}\rho(p_l^{m-1})) \qquad (14)$$

In the usual non cavitated case, the terms ρ(p) are known and the value of p_k^m *is* immediately obtained from (14). In the present situation only the terms for (l) different from (k) are known , so that it is not possible to conclude directly for the value of p_k^m .

Putting in evidence the unknown terms , (14) can be rewritten as:

$$p_k^m = D/a_{k,k} + b_{k,k}\rho(p_k^m)/a_{k,k} \qquad (15)$$

With

$$a_{k,k} = (\left[\frac{\rho(p)}{12\mu(p)}h^3\right]_{k-1/2}^{m-1} + \left[\frac{\rho(p)}{12\mu(p)}h^3\right]_{k+1/2}^{m-1}) \qquad (16)$$

$$D = p_{k+1}^m(\left[\frac{\rho(p)}{12\mu(p)}h^3\right]_{k+1/2}^{m-1} + p_{k-1}^m(\left[\frac{\rho(p)}{12\mu(p)}h^3\right]_{k-1/2}^{m-1} + \frac{u}{2}\Delta x[\rho(p)h]_{k-1}^m \qquad (17)$$

$$b_{k,k} = -\frac{u}{2}\Delta x[h]_k^m \qquad (18)$$

Due to the choice (10a) of discretization , $b_{k,k}$ is non-negative and $a_{k,k}$ is less than zero for finite element or finite difference P1 usual upwind discretization. From figure (2) it is easy to show that there is only one value p_k^m which is solution of (15): the intersection of the pressure density curve and of a straight line. Depending on the actual values of D, $a_{k,k}$ and $b_{k,k}$ there are 3 possibilities , two of which are easily computed while supplementary computations can be necessary in the last case.

case(a): the solution is in the pure vapor region. From equation (4a) the pressure solution Prop1 of (15) is defined by:

$$\text{Prop1} = D/(a_{k,k}(1-b_{k,k})/(a_{k,k}c_v^2))) \qquad (19a)$$

Case (b): The solution is in the pure liquid region . From (4b), the pressure solution Prop2 of (15) is defined by:

$$\text{Prop2} = (D/a_{k,k} + b_{k,k}/(a_{k,k}(\rho_l - P_{sat}/c_l^2)))/(1-b_{k,k}/(a_{k,k}c_l^2)) \qquad (19b)$$

Case (c): The solution Prop3 is in the mixture region. From (4c), the pressure Prop3 satisfies the non-linear equation (20):

$$\text{Prop3} = \frac{(\rho_l \rho_v^2 \mathrm{c}_\mathrm{v}^2 - \rho_l^3 \mathrm{c}_\mathrm{l}^2)\mathrm{e}^{(\text{Prop3}-\mathrm{p}_\mathrm{sat})/\mathrm{N}}}{(\rho_v \mathrm{c}_\mathrm{v}^2(\rho_\mathrm{v} - \rho_l) - (\rho_l^2 \mathrm{c}_\mathrm{l}^2 - \rho_l \rho_\mathrm{v} \mathrm{c}_\mathrm{v}^2)\mathrm{e}^{(\text{Prop3}-\mathrm{p}_\mathrm{sat})/\mathrm{N}}} \qquad (19c)$$

This last equation can be solved by a Newton procedure or a dichotomy one. It will be seen later that this step can be shortened by taking a linear approximation of (4c).

As soon as these three possible solutions have been computed , it suffices to verify which is the one which is compatible with the actual choice of the pressure:

If Prop1 is less than p_{vm}, it is the actual solution of (15) and p_k^m =Prop1; if Prop2 lies between p_{vm} and p_{sat}, then p_k^m =Prop2 , else p_k^m =Prop3. Due to the monotonicity of the pressure-density curve there is only one possibility.

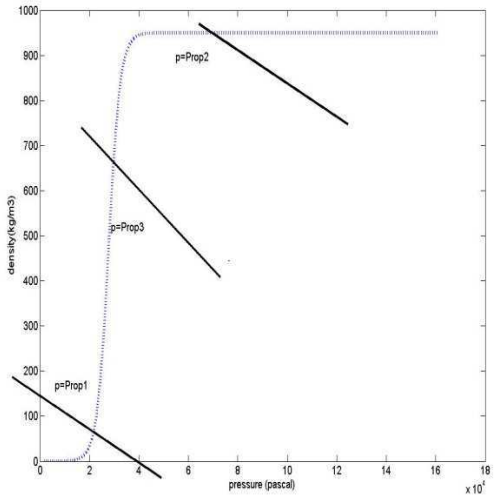

.

Figure2: Computation of the solution of the implicit equation: The three possibilities

3.3 Application to the solution of the J.F.O./E.A cavitation model

Usual JFO models are defined up to a unique parameter, the cavitation pressure p_{cav}. There are described by a two unknowns problem (pressure p and relative proportion of fluid θ) given by the following Reynolds equation:

$$\frac{\partial}{\partial x_1}\left(\frac{h^3}{12\mu_l}\rho_l\frac{\partial p}{\partial x_1}\right)+\frac{\partial}{\partial x_2}\left(\frac{h^3}{12\mu_l}\rho_l\frac{\partial p}{\partial x_2}\right)=u/2\frac{\partial(\theta\rho_l h)}{\partial x_1}+\frac{\partial(\theta\rho_l h)}{\partial t} \qquad (20)$$

And the additional constraint:

$$p\geq p_{cav},\ 0\leq\theta\leq 1,\ (p-p_{cav})(\theta-1)=0 \qquad (21)$$

This is equivalent to say that P obeys a Reynolds compressible equation such that the density pressure relation is defined by the Heaviside function:

$$\rho(p)=\rho_l \ if\ \ p\geq p_{cav} \quad 0\leq\rho(p)\leq\rho_l \ if\ \ p=p_{cav} \qquad (22)$$

So that $\theta\rho_l$ can be identified to $\rho(p)$ in the cavitation area.

Elrod and Adams introduce some compressibility effect in the non cavitated area, using the additional bulk parameter β . Also this is equivalent to solving Reynolds compressible equation with a slightly different pressure density law (see figure 2 and equation (15) in [4]):

$$\rho(p) = \rho_l \, e^{(p-p_{cav})/\beta} \;\; if \;\; p \geq p_{cav} \quad 0 \leq \rho(p) \leq \rho_l \;\; if \;\; p = p_{cav} \qquad (23)$$

Later on , Sahlin et all proposed to use other compressibility laws in the non cavitated area, like the Dowson Higginson one [16].

The pressure-density law (23) is an approximation of the one defined by (22)and the solution of the E.A model tends to the solution of the JFO model for large values of β. Alternatively, it can be said that J.F.O. law (21) is an approximation of the more realistic E.A. law approximation (23), approximation which is valid for large β. Even if the actual value of the bulk compressibility is not known, a sufficiently large value of this parameter can be chosen. The idea being that the problem using compressibility law (23) is numerically easier to solve than the actual J.F.O. one (22).

In the same way, starting from the J.F.O. model in which p_{cav} is the only data related to the cavitation phenomenon, we propose to introduce an approximate density law which has the overall characteristics of the J.F.O. compressibility law and for which the computation is easier:

Fully compressible law(4) is a possible candidate for this approximation. It however needs 6 additional parameter to be known or chosen (density , sound velocity, viscosity). Moreover, solving (19c) to obtain Prop3 requires some additional computations. We propose to use a simpler law which needs only two additional parameter p_{Inf} and ρ_{inf} for which the solution of (19c) is now obvious :

$\rho(p)= \rho_{inf}$ if $p< p_{\inf}$; $\rho(p)= \rho_l \, (p- p_{\inf})/(p_{cav} - p_{\inf}) + \rho_{inf}$ if $p_{\inf} <p< p_{cav}$; $\rho(p)= \rho_l$ if $P> p_{cav}$ (24)

In which $p_{\inf}$ is a parameter to be chosen between 0 and p_{sat} to mimic p_{vm} .

Due to the simplicity of this law in the 3 regions, the 3 possible solutions of the implicit algorithm are easy to compute (no Dichotomy or Newton method is requires to compute Prop3)

Prop1= $(D + b_{k,k}\rho_{\inf}) / a_{k,k}$ (25a)

Prop2= $(D + b_{k,k}\rho_l) / a_{k,k})$ (25b)

Prop3= $\left[(D + b_{k,k}\rho_{\inf}\ )\ (p_{sat} - p_{\inf}\ \ - b_{k,k}\rho_l\ P_{\inf}\ \right] / \left[a_{k;k}\,(p_{sat} - p_{\inf}) - b_{k;k}\rho_l\right]$ (25c

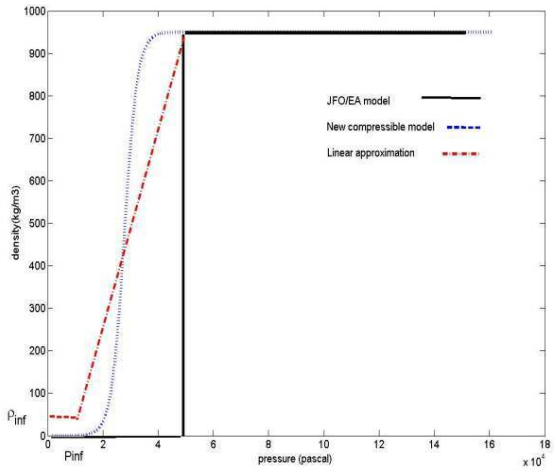

Figure 3: Three pressure-density laws: JFO/EA model , full compressible model and linear approximation model

4 Numerical applications in steady state situations

Various kinds of numerical results will be presented .

-The first one is for an infinitely long parabolic slider bearing (Variations along the x_2 variable are neglected) with data issued from the paper of Sahlin et all[16]

- The second for a twin slider bearing to mimic roughness . It allows to emphasis differences between conservative and non-conservative models and between fully compressible model and J.F.O./E.A . model for low pressure.

- The last one is a journal bearing with large eccentricity

4.1) Example1 [16].

Geometrical and cinematic data are issued from [16]. Rheological data have been chosen to get transition pressures P_{sat}=0.6 bar and P_{vm}=0.02 bar and are given in Table1 . The viscosity is assumed to be the same in all regions.

The full explicit algorithm has been applied using a Gauss -Seidel over relaxation procedure with a relaxation factor ω=1.92 for various number M of nodes with boundary conditions Pext= 1 bar. The results are given in table 2 : Load W, input mass flow Qi, outputmass flow Qo, maximal pressure p_{max} and relative error I IP^m-P^{m-1}II/IIP^mII at the last iteration:

$$W = \int_0^L (p - P_{ext})dx \tag{26}$$

$$QI = -\frac{h(0)^3 \rho(0)}{12\mu}\frac{dp}{dx}(0) + \frac{\rho(0)h(0)u}{2} \quad Q0 = -\frac{h(L)^3 \rho(L)}{12\mu}\frac{dp}{dx}(L) + \frac{\rho(L)h(L)u}{2} \tag{27}$$

Let us observe that the mass conserving property is not preserved unless taking great number of nodes. This is due to the oscillations of the solution in the cavitation area. These oscillations prevent the diminution of the error for small number of nodes: The error slowly decreases and oscillates . Even if the error becomes small, there still exist some oscillations which prevent a good computation of the mass flow in the cavitation area. It is necessary to choose M>2000 to obtain an error on the mass flow less than 10%.

Velocity m/s	μ_v (Pa.s)	μ_l (Pa.s)	$c_{v(m/s)}$	c_l (m/s)	ρ_v (kg/m3)	ρ_l (kg/m3)	L(m)	h_{max} (m)	$h_{min(m)}$
4.57	0.0039	0.039	352	1600	0.950	0.019	0.0762	$5.08x10^{-5}$	$2.54x10^{-5}$

Table1: journal bearing data. Example1

Computation has been made with discretization (10b) of the right hand side, other discretization's lead to a blow up (the computed terms tend to infinity).

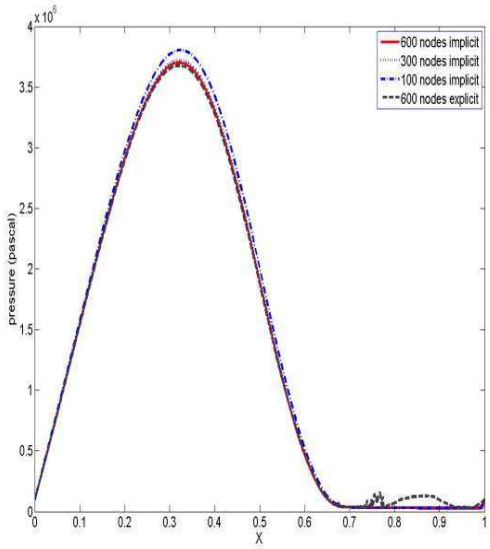

Figure 4 : Pressure fied : A comparison between explicit and implicit algorithms

Figure 4 shows clearly that the oscillations are restricted to the cavitation area so that if we are interested only by the value of the load, it is not necessary to use a great number of nodes.

Table 3 gives some results using this implicit procedure with the same data used for the explicit method.

The convergence is a regular one and the error is decreasing, enabling us to use a classical test to limit the number of iterations. The mass flow conservation is satisfied as soon as M is greater than 300. As it is clear from figure 4 , there is no oscillations and even the result with M=100 is a good overall approximation of the solution.

Remark 4.1: The present procedure can be compared with the usual Christopherson procedure to deal with Reynolds cavitation model with constraint $p>p_{sat.}$. As it is shown in the appendix, both algorithms have the same structure and differ only a few lines. To obtain the Christopherson solution, it suffices to choose p^m_i =max (Prop2, p_{sat}).

Remark 4.2: In such a problem, there are two kinds of numerical errors . The first one E1 is linked to the discretization and the fact that the finite dimensional problem we want to solve is not the exact continuous one . The second one E2 is the error between the actual computed solution and the theoretical one of the discretized problem. For a given problem and a given method E1 is essentially a function of the number of nodes and E2 of the number of nodes M and number of iterations. To estimate the minimal number of nodes required , we choose as a criteria the difference between the input mass flow and the output mass flow. To get an error on the input mas flow less than 1%, it is necessary to get M>400. It is also shown that the load,the maximal pressure and the mass flow are stabilized as soon as I IP^m-P^{m-1}II/IIIP^mII is less than 10^{-7} . This value is chosen to stop the iterations.

M	P_{max}(bar)	Qi kg/s	Qo kg/s	Relative error for the last 1000 iterations	Load W N/m	nmax
600	38	0.062	0.099	Between 2.5×10^{-3} and 1.3×10^{-2}	107	6000
900	36.6	0.062	0.091	Between 10^{-3} and 2.4×10^{-3}	98	6000
1200	36	0.063	0.086	Between 5.7×10^{-4} and 6.1×10^{-4}	96	7000
2000	35.8	0.063	0.073	Between 10^{-4} and 2×10^{-4}	96.5	22000
3000	35.4	0.063	0.063	3.6×10^{-5}	94.3	40000

Table2: Computed journal bearing parameters . Example1. Explicit algorithm

M	P_{max}(bar)	Qi kg/sm	Qo kg/sm	Number of iterations to have an error less than 5×10^{-7}	Load W N/m
100	38	0.061	0.086	200	103
300	37.2	0.062	0.062	650	100
600	37	0.062	0.062	2400	99.5

Table3: Computed journal bearing parameters . Example1. Implicit algorithm

More detailed comments will be given in section 6.

Remark 3.3: The solution of equation (19c) has been obtained by a dichotomy method with 15 level of bisections . This number allows to get a good approximation of the solution. A too low number of bissections (10 for example) does not modify the load and maximal pressure but induces a bad computation of the mass flow .

4.2 Example 2: A twin parabolic slider bearing.

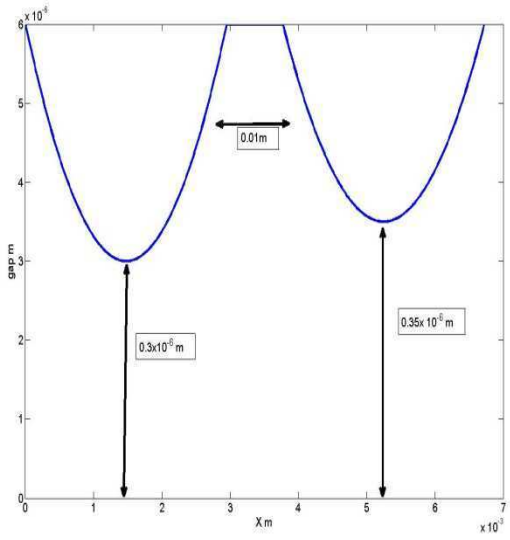

Figure5: Twin slider gap

The following data has been chosen to mimic some roughness aspect of a lubricated device and to emphasis the difference between various algorithms. The device is made of two successive parabolic slider of length 0.036 m separate by a flat surface of 0.01m (see fig5). The minimal gap is 3x 10^{-6} m for the first slider, 3.5 x10^{-6} m for the second slider . The maximal gap is 6 x10^{-6} .

Various models have been compared:

- The present implicit algorithm proposed in section 3.2 when using all the known parameters of the fluid (ρ_v, ρ_l , c_v, c_l ,μ_v,μ_l) . Data for the fluid are identical to the table 1 so that p_{sat}=0.60 bar and p_{vm} =0.023 bar.

-The Christopherson algorithm (Reynolds model with $p_{cav} = p_{sat}$, constant density ρ_l and viscosity μ_l))

- The modified one to mimic the J.F.O./E.A. model using linear law (25). In this case, two additional parameters p_{inf} and ρ_{inf} are needed . Various choices are proposed for p_{inf} from $p_{inf} = p_{vm}$ to $p_{inf} = 0.99\ p_{sat}$ In the last case the linear density -pressure curve between p_{inf} and p_{sat} is close to the vertical curve of the J.F.O./E.A. model (An other choice like $p_{inf} = 0.999\ p_{sat}$ does not change any results). Concerning ρ_{inf} , it has been chosen equal to zero or the "exact value'" $\rho_{v.}$ Results are given in Tables 3and 4 respectively with a velocity u=5m/s and u=2m/s, 400 nodes of discretization and an over relaxation coefficient ω=1.9.In Figure6 the pressure curves for the Christopherson model, the full compressible one and the linear one(25) are presented for u=2m/s. Pressure curves for other linear approximation models lie between the two last curves.

For each computation, minimum and maximum values of the pressure, input and output mass flow, load and number of iterations to get the relative error of 10^{-8} are given.

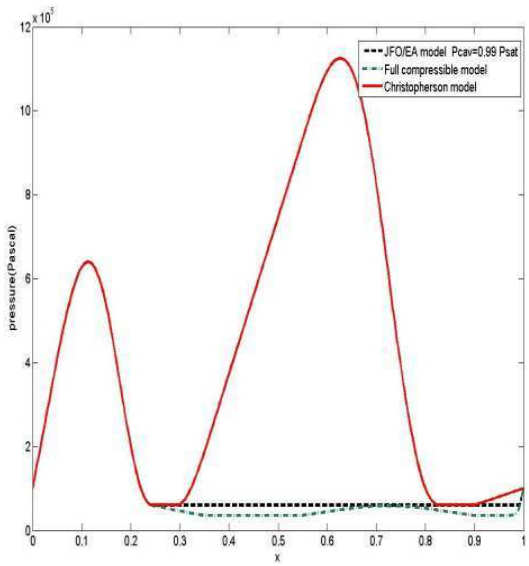

Figure6: Twin Slider bearing: Pressure fields. Comparison of various models

U=5m/s M=400nodes	ρ_{inf} kg/m^3	P_{inf} bar	Min(p) bar	Max(p) bar	Qi Kg/ms	Q0 Kg/ms	Load N/m	Number of iterations to have an error less than 10^{-8}
Full compressible	0.019	0.023	0.28	14.48	0.079	0.080	12 376	900
Linear Approximation(1)	0.019	0.023	0.35	14.53	0.0793	0.0807	13 551	518
Linear approximation(2)	0.	0.023	0.35	14.53	0.0793	0.0805	13 547	493
Linear approximation(3)	0.019	0.599	0.60	14.53	0.0793	0.0807	14 842	458
Linear appro.(4) (JFO/EA model)	0	0.599	0.60	14.53	0.0793	0.0804	14 841	458
Linear approximation(5)	0	0.55	0.58	14.53	0.0793	0.0804	14 724	458
Reynolds model			0.60	27.25	0.0793	0.141	87 991	1200

Table 4. Twin slider (example2) Computed Journal bearing parameters . moderate pressure u=5m/s

Implicit algorithm

U=2m/s M=400 nodes	ρ_{inf} kg/m^3	p_{inf} bar	Min(p) bar	Max(p) bar	Qi Kg/ms	Q0 Kg/ms	Load N/m	Number of iterations to have an error less than 10^{-8}
Full Compressible	0.019	0.023	0.28	6.29	0.319	0.0324	1 420	1600
Linear app.(1)	0.019	0.023	0.35	6.35	0.0318	0.0323	2 613	1184
Linear approximation(2)	0.	0.023	0.35	6.35	0.0318	0.0323	2 609	1200
Linear approximation(3)	0.019	0.599	0.60	6.35	0.0318	0.0323	3 882	453
Linear approxi.(4) (JFO/EA model)	0	0.599	0.60	6.35	0.0318	0.0323	3 882	453
Linear approximation(5)	0	0.55	0.58	6352	0.0318	0.0323	3766	458
Reynolds model (Christopherson algorithm)			0.60	11.25	0.0318	0.055	33 261	1200

Table 5. Twin slider (example2) Computed Journal bearing parameters .low pressure u=2 m/s

Implicit algorithm

The figure6 explains the results of table4.(same explanations are valid for table3):

- All models have a first pressure 'hump' which are nearly identical . For the linear models and the full compressible one , the input mass flow is not sufficient to induce a second pressure hump. However the Reynolds-Christopherson model implicitly prevents (see[7]) the cavitation taking place in a convergent gap , hence the presence of the second pressure hump and the important difference between the loads. Such a phenomenon has already been mentioned and its importance when roughness takes place has been studied in [18].

- Results obtained by linear approximation (25) are identical with results obtained for another cavitation algorithm proposed in [19]. It is noteworthy that even a choice of $p_{inf} = 0.9\ p_{sat}$ in linear model (25) which corresponds to a density-pressure curve without a vertical part gives a good approximation for the J.F.O./E.A. model. This result numerically justifies the proposed implicit algorithm to solve the J.F.O./E.A. model.

- Differences between linear models are mainly due to the choice of p_{inf} ,not to the choice of ρ_{inf} . The difference between the number of iterations required is mainly the consequence of the fact that the maximal pressure is greater for the Christopherson model and that the optimum relaxation parameter are not the same for the various models. Recall that the optimum relaxation parameter is associated to the number of nodes in the non-cavitated area which is different following the models used.

-The difference of the loads between the linear approximations and the full compressible models is mainly due to the existence of under-pressure in the full compressible model . This does not change maximal pressure and mass flow. As the overall pressure is small and the cavitation covers near ¾ of the surface of the device, this importance is exacerbated especially for u=2m/s (Table 5). For overall larger pressure (Table 4, u=5m/s), the difference is smaller.

4.3 Example 3 : A large eccentricity journal bearing.

The third example shows that the stability property of the linear compressible approximation is still valid for large pressures. The device is a journal bearing of radius R=0.05m , width=0.02m, eccentricity=0.95 and radial clearance 75x 10^{-6}m, velocity 5m/s , supply pressure 2bar (left hand side of figure7) and open-end pressure (right hand side of figure 7)is 1 bar. Viscosity μ_l=0.03 Pa.s . Rheological data are such that p_{sat}=0.6bar and p_{vm}=0.02bar

The solution of the J.F.O./E.A. has been first computed (level curves with continuous line on Fig 7). Then the linearized compressible model has been computed (level curves with dotted lines)with additional parameters ρ_{linf}=0.0 and p_{inf}=0.02 Bar (cf equation 25)). Differences for the maximal pressure and load are less than 1/1000. Level curves for pressures greater than 2 bar are superimposed . The only difference is the location of the level curves for pressure less than one bar. As a consequence, the cavitation areas (defined by the level curves for pressure=p_{sat}) are slightly different . This however does not change the values of the operational parameters for the bearing. Note that the minimum pressure is 0.04 bar in the fully compressible mode (marked by a small circle in figure 7) under the saturation pressure..

Choosing p_{inf} =0.54 bar (90%of the value of p_{sat}) leads to a solution closer to the J.F.O./E.A. model even in the divergent part of the bearing . The minimal pressure is 0.57 bar (only 0.03 bar below the saturation pression) . At last choosing p_{inf} =0.99 p_{sat} leads to a solution identical to the one of the J.F.O./E.A. model.

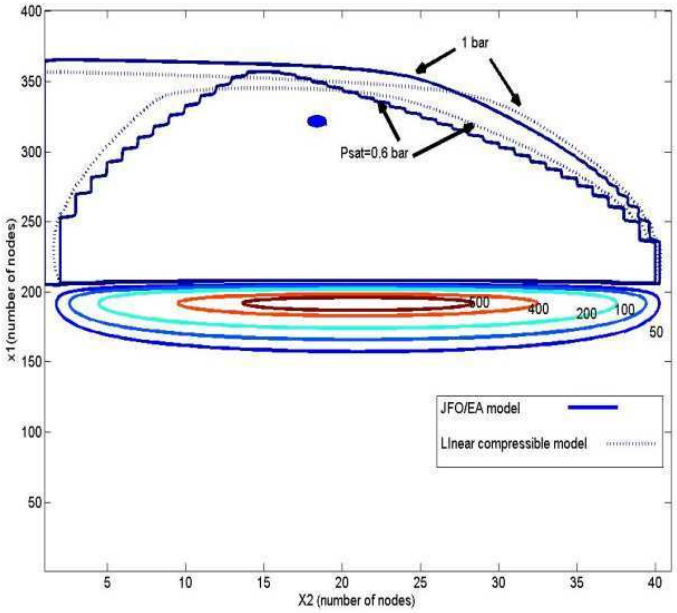

Figure7: Journal bearing: Pressure field. A comparison between JFO/EA model and compressible linearized model

5 Algorithm for unsteady problem.

5.1 As mentioned in section 2 , the fully compressible theory is also valid for dynamical situations.. It is possible to generalize the (half) implicit method defined in section 3.2 to such situations.

Let us perform first an implicit time discretization in Reynolds equation (2) with time step Δt. At each time n Δt , we have to compute $p^n(x)$ such that :

$$\frac{\partial}{\partial x_1}\left(\frac{[h^3]^n}{12\mu(p^n)}\rho(p^n)\frac{\partial p^n}{\partial x_1}\right)+\frac{\partial}{\partial x_2}\left(\frac{[h^3]^n}{12\mu(p^n)}\rho(p^n)\frac{\partial p^n}{\partial x_2}\right)= \\ = u/2\,\frac{\partial(\rho(p^n)[h]^n)}{\partial x_1}+\frac{\rho(p^n)[h]^n-\rho(p^{n-1})[h]^{n-1}}{\Delta t} \qquad (28)$$

Exactly as in the steady state situation, a finite element or finite difference discretization can be used.

At each time step, a nonlinear system is to be solved . Its general row is written as (for a one dimensional space dimension for sake of simplicity):

$$p_{k+1}^{n}\left(\left[\frac{\rho(p)}{12\mu(p)}h^3\right]_{k+1/2}^{n}+p_{k-1}^{n}\left(\left[\frac{\rho(p)}{12\mu(p)}h^3\right]_{k-1/2}^{n}+\frac{u}{2}\Delta x[\rho(p)h]_{k-1}^{n-1}\right.\right. \tag{29}$$
$$=\frac{u}{2}\Delta x[\rho(p)h]_{k}^{n}+p_{k}^{n}\left(\left[\frac{\rho(p)}{12\mu(p)}h^3\right]_{k-1/2}^{n}+\left[\frac{\rho(p)}{12\mu(p)}h^3\right]_{k+1/2}^{n}\right)+\frac{[h\,\rho(p)]_{k}^{n}-[h\,\rho(p)]_{k}^{n-1}}{\Delta t}(\Delta x)^2$$

This system is solved by a fixed point iterative method of index m. As for the steady state problem, a linearization is performed at each step of this fixed point procedure for the coefficients $\rho(p)/12\mu(p)$ of the left hand side of this equation :

For fixed time step index n, $\{p^n\}$is the limit as m tends to infinity of a sequence $\{p^{n,m}\}$such that each component $\{p_k^{n,m}\}$is defined by :

$$p_{k+1}^{n,m}\left(\left[\frac{\rho(p)}{12\mu(p)}h^3\right]_{k+1/2}^{n,m-1}+p_{k-1}^{n,m}\left(\left[\frac{\rho(p)}{12\mu(p)}h^3\right]_{k-1/2}^{n,m-1}+\frac{u}{2}\Delta x[\rho(p)h]_{k-1}^{n,m}\right.\right. \tag{30}$$
$$=\frac{u}{2}\Delta x[\rho(p)h]_{k}^{n,m}+p_{k}^{n,m}\left(\left[\frac{\rho(p)}{12\mu(p)}h^3\right]_{k-1/2}^{n,m-1}+\left[\frac{\rho(p)}{12\mu(p)}h^3\right]_{k+1/2}^{n,m-1}\right)+\frac{[h\,\rho(p)]_{k}^{n,m}-[h\,\rho(p)]_{k}^{n-1,m}}{\Delta t}(\Delta x)^2$$

Exactly as in the steady state case, this equation can be rewritten as :

$$p_k^{n,m}=D/a_{k,k}+b_{k,k}\rho(p_k^{n,m})/a_{k,k} \tag{31}$$

With:

$$a_{k,k}=\left(\left[\frac{\rho(p)}{12\mu(p)}h^3\right]_{k-1/2}^{n,m-1}+\left[\frac{\rho(p)}{12\mu(p)}h^3\right]_{k+1/2}^{n,m-1}\right)$$

$$D=p_{k+1}^{n,m}\left(\left[\frac{\rho(p)}{12\mu(p)}h^3\right]_{k+1/2}^{n,m-1}+p_{k-1}^{n,m}\left(\left[\frac{\rho(p)}{12\mu(p)}h^3\right]_{k-1/2}^{n,m-1}+\frac{u}{2}\Delta x[\rho(p)h]_{k-1}^{n,m}+\frac{[h\,\rho(p)]_{k}^{n-1,m}}{\Delta t}(\Delta x)^2\right.\right.$$

$$b_{k,k}=-\frac{u}{2}\Delta x[h]_{k}^{n,m}-\frac{[h\,]_{k}^{n,m}}{\Delta t}(\Delta x)^2 \tag{34}$$

This equation has exactly the same structure as equation (15). The solution is obtained by choosing between the 3 possibilities defined by equation (19 if using "exact" pressure-density law or (25) using the approximate J.F.O./E. A . model.

5.2 Numerical example

This example has been proposed by Optasanu and Bonneau in [19] and has been also used by Giacopini and all [13]: Two rigid plates, infinitely large are separated by a thin film of oil and are fully immerged in a lubricated bath at pressure p_{ext}. The lower one is fixed and the upper one has a parabolic shape . The two plates are moved apart and then brought together in a cyclical manner. The film thickness is given by:

$$h(x,t)= h_0-h_1\cos(\omega t)+a\, x^2$$

with : $0<x<0.0462$m , $a=10^{-10}$m, $h_0= 19.8\text{x } 10^{-6}$m, $h_1= 18.15\text{x } 10^{-6}$m, $\omega= 10.47$rd/s $p_{ext}=10.6$bar

At time t=0, the fluid is assumed continuous (no cavitation area) and at the constant pressure P_{ext}.

A cavitation region appears at the center of the plates when they move away and disappears during the squeezing process. Analytic solutions have been obtained by Optasanu and Bonneau's for the JFO /EA model.

Figure(8) shows the variation in time of the relative density of the fluid $\rho(p)/\rho_l$ at the center of the plates for various values of the time step δ and number of nodes M. At each time step, computations have been made with the linearized full compressible model (25) with $p_{sat}=0.6$ bar, $p_{inf}=0.99p_{sat,}$ $\rho_{inf}=0$, $\rho_l=950$ kg/m^3 and constant viscosity 0.005 Pa.s. Note that in [19] the value of $p_{cav}=0$,so that we have to choose $p_{ext}=10.6$ in the present cavitation to maintain the difference p_{ext}-p_{cav} at the same value.

For small value of M, an exact solution is obtained for a time step of 0.002s. However ,as soon as M increases , the time step necessary to obtain a good approximation of the exact solution must be

smaller. For M= 400, a time step smaller than 0.001s is necessary. Let us mention also that the jump for the density just before the reformation time is obtained for M>200 in only one time step.

The following sequence of figures (9)(10)(11) describe for the same device the minimum pressure, maximum pressure and load for the Christopherson algorithm, two linearized compressible model (p_{inf}=0.99 p_{sat} and p_{inf}=p_{vm}). and a full compressible one (computations for M=200, δ=0.01s). Clearly, once more the Christopherson solution is very different from the results of the other computations . These three others computations show a difference for the pressure which is essentially limited to the low pressure situation so that load curves are superimposed at any time. This confirms the good stability of the computational procedure with respect of the numerical parameters describing the cavitation via the pressure-density law.

6 **Acceleration of the convergence .**

It is possible to accelerate the convergence of the algorithm by using an successive-over-relaxation procedure (S.O.R.) with parameter ω which lies between 1 and 2, exactly as the one used in [2] for the Reynolds cavitation model. Due to the hyperbolic feature of the Reynolds equation in the "cavitated area", this over-relaxation procedure has to be used only for the nodes inside the pure liquid region.

In order to do that, the solution p_k^m is not directly computed by using Prop2 in equation (19b) . It is given by;

$$p_k^m = \text{Prop2} * \omega + (1-\omega) * p_k^{m-1}$$

The optimum value of the parameter ω is essentially function of the number of modes M as illustrated in Tables 6 and 7 . These tables give the number of iterations required to obtain a relative error of 10^{-7} for the pressure, respectively for example2 and example3 as a function of the parameter ω. Computations have been made for various discretizations. At this level of

convergence, all parameters (load, attitude angle , input, output mass flow) are stabilized and are the same for each row (the error E2 defined in remark 4.1 is negligible).

The penultimate column gives the relative difference between input and output mass flow values for each computation. The last column gives the relative difference between the “exact “ value of the load computed with M=1500 for example 2 (M=750x50 for example 3) and the load computed for the value of current M .

These results show that for M<500,(example2) it is impossible to obtain a correct computed mass flow balance (less than 1%), even with a very good convergence for the pressure . In other words the error E1 defined in remark 4.2 is preponderant.

These results also show that the influence of ω for this problem is exactly the same than as solving linear problems :

-The optimum value increases usually with the number of nodes.

-The time of computation can be divided by 4 or 5, compared to the case without the over relaxation procedure (corresponding to ω=1)

-It is better to underestimate the optimal value than to overestimate it (even for a small value)) as the increase of the number of iterations can be very important and leads to a divergent sequence. For practical use it is not necessary to compute exactly the optimal parameter : In example 3 the choice ω=1.6 gives a good improvement in computational time for all kind of discretization’s .

-For 2-dimensional problems (example3), not only the total number of nodes is important, but also the ratio of the nodes in each of the direction. The number of iterations is minimal as the ratio of the discretized element: $\Delta x_1 / \Delta x_2$ is the same as the ratio: Perimeter/width of the bearing. This is not however the only parameter to deal with. As illustrated in Table7, the error on the load (he actual one and the “exact one” computed for M= 750x50) is smaller for M= 400x10 (ratio $\Delta x_1 / \Delta x_2$=40) than

for M= 250x16 (ratio$\Delta x_1 / \Delta x_2$=15) which is the optimal ratio. This is due to the anisotropy of the problem . The error E1 is smaller in the first case than in the second one.

Example 2	ω=1	ω=1.8	ω=1.9	ω=1.98	ω=1.99	ω=1.999	Mass-flow error	Load error
M=100	485	**93**	139	687	1351	>10000	20%	25%
M=400	5746	1317	1148	**997**	1280	>10000	1.5%	6%
M=600	1>10000	2894	2498	2156	**2109**	>10000	1.1%	3%
M=1000	>10000	8136	6904	5737	5520	**9302**	0.15%	1%

Table 6: Influence of the over relaxation parameter -1d problem . Example2. Number of iterations requires to obtain a relative error of 10^{-7} on the pressure and relative errors for load and mass-flow.

Example3	ω =1	ω =1.6	ω =1.65	ω =1.7	ω =1.72	ω =1.8	1.85	1.9	Mass flow error	Load error
M=400x10	675	188	168	154	149	133	**124**	143	5%	1%
M=250x16	474	130	117	107	103	**91**	92	div	2%	5%
M=200x20	518	140	125	**112**	**112**	137	div		1.2%	8%
M=800x20	>2000	663	574	498	475	415	385	**360**	1.3%	0.5%
M=500x32	1670	468	405	353	340	296	**275**	div	0.6%	1%
M=400x40	1817	530	440	381	**363**	div			0.15%	3.6%

Table 7: Influence of the over relaxation parameter -2d problem . Example3. Number of iterations requires to obtain a relative error of 10^{-7} on the pressure. (grey boxes means divergence)

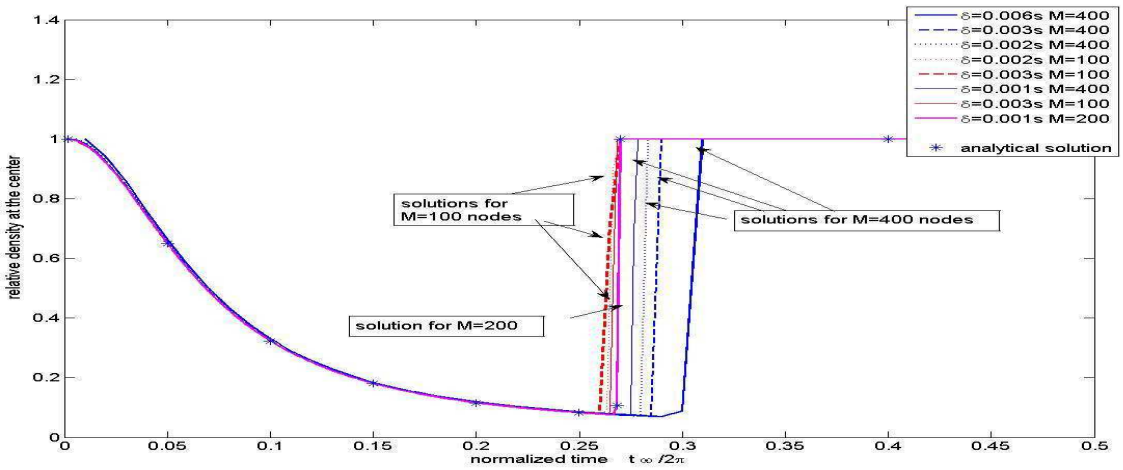

Figure 8 : Squeeze field bearing: History of the relative density at the center of the plate versus time

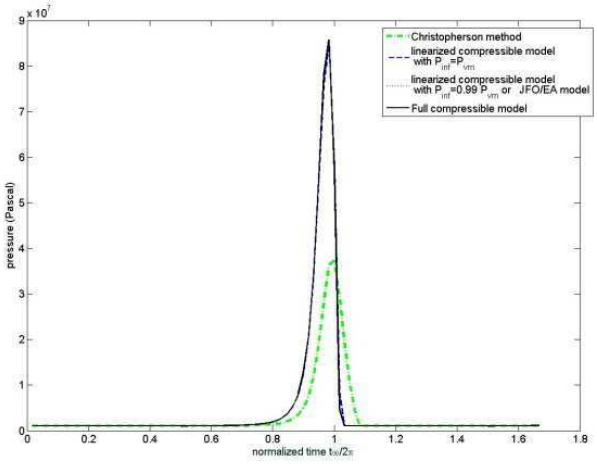

Figure 9: Squeeze field bearing: Maximal pressure versus time

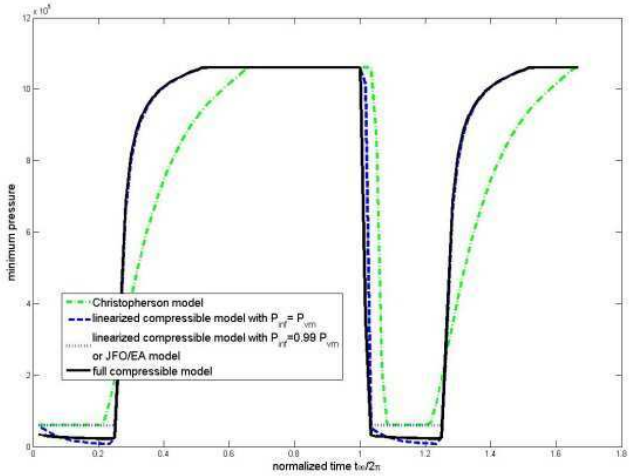

Figure 10: Squeeze field bearing: Minimal pressure versus time

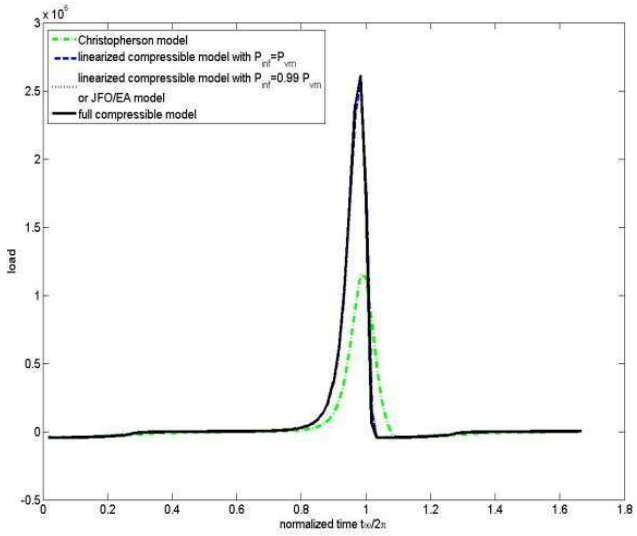

Figure 11: Squeeze field bearing; load versus time

7 **Conclusion:** The fully compressible model recently proposed to deal with vaporous cavitation is very close to the usual mass flow conservation Jakobson-Floberg-Olsson/Elrod-Adams model. However it is easier to solve due to the fact that positivity of the pressure is not required. Two algorithms are proposed for this new model. A first one which is based on a sequence of resolutions of linear systems requires a relatively great number of nodes to prevent oscillations. A second one, although retaining the non linear aspect of the problem is

easy to implement. It is very similar to the well-known Christopherson algorithm with a Gauss-Seidel over relaxation parameter. The most important feature is that the non linear discrete equation can be exactly solved at each iteration. Introduced first for steady state problem, it is shown how it can be extended to unsteady problems. Moreover it can be also used to solve the J.F.O./E.A. cavitation model by approximating the J.F.O./E.A density-pressure curve by a linear approximation. The time computation can be greatly reduced by using a successive- over-relaxation procedure.

[1] Dowson D , Taylor CM. Fundamental aspects of cavitation in bearings," in *Cavitation and related phenomena in lubrication,* Mechanical Engineering Publications for the Institute of Tribology, The University of Leeds,1975; pp. 15-25.

[2] Christopherson DG. A new mathematical method for the solution of film lubrication problem. Inst. Mech. Eng. Proc. 1941;146:126-135.

[3] Jakobsson B, Floberg L. The finite journal bearing considering vaporization. Göteborg: Transactions of the Chalmers University Technology 190; 1957.

[4] Elrod HG, Adams L. A Computer program for Cavitation and Starvation. *In: Dowson, Godet, Taylor, editors. Cavitation and related phenomena in lubrication*, Mechanical

Engineering Publications for the Institute of Tribology, The University of Leeds; 1975, p. 37-41.

[5] Etsion L, Ludwig LP. Observation of Pressure variation in the Cavitation region of submerged Journal bearings. Journal of Lubrication Technology 1982; 104: 157-163.

[6] Braun MJ, Hendricks RC. An experimental Investigation of the Vaporous/Gaseous Cavity Characteristics of an Eccentric Journal Bearing, ASLE Transactions 1983; 27(1):1-14.

[7] Bayada G, Chambat M. Analysis of a free boundary problem in partial lubrication. Quartely Applied Math. 1983; 40(4):369-375.

[8] Vijayaraghavan D, Keith Jr. An efficient, robust and time accurate Numerical Scheme applied to a cavitation algorithm. Journal of Tribology 1990; 112: 42-51.

[9]Kumar A, Booker JF. A finite Element cavitation Algorithm: Application and Validation. Journal of Tribology 1991;113: 255-261.

[10] Vincent B, Maspeyrot P, Frêne J. Starvation and cavitation effects in finite journal bearings. In : D. Dowson et al editors. Leeds Lyon Symposium on Lubricants and Lubrification, Elsevier Science Tribology series, 30;1995, p. 455-464.

[11] Bayada G, Chambat M, Vázquez C. Characteristics method for the formulation and computation of a free boundary cavitation problem. Journal Computing and Applied Math. 1988; 98 (2):191–212.

[12]Alvarez,SJ, Oujja R. A new numerical approach of a lubrication free boundary problem. Applied Math. and Computation 2004;148(2):393-405.

[13] Giacopini M, Fowell MT, Dini D , Strozzi A. A Mass-Conserving Complementarity Formulation to Study Lubricant Films in the Presence of Cavitation. Journal of Tribology 2010; 132, 702-714.

[14] Chupin L, Sart R. Compressible flows: New existence results and justification of the Reynolds asymptotic in thin film. Asymptotic Analysis 2012;76(3-4):193-231.

[15] Bayada G, Chupin L. Compressible fluid model for hydrodynamic lubrication cavitation. Journal of Tribology 2013;To appear. J.F.O./E.A

[16] Sahlin F, Almquist A, Larsson R, Glavatskih S. A cavitation algorithm for arbitrary lubricant compressibility. Tribology International 2007;40:1294-1300.

[17] Ausas R, Jai M, Buscaglia GC. A mass-conserving algorithm for dynamical lubrication problems with cavitation. Journal of Tribology 2009;131:031702-1.

[18] Ausas R, Ragot P, Leiva J, Jai M, Bayada G, Buscaglia GC. The impact of the cavitation model in the analysis of a microtextured lubricated journal bearing. Journal of Tribology 2007;129(3):868-875.

[19] Optasanu V, Bonneau D. Finite Element mass-conserving cavitation algorithm in pure squeeze motion: Validation/application to a connecting-rod small end bearing. Journal of Tribology 1986;122: 162-169.

Appendix : Detailed algorithm for steady state situation. A comparison between the present linearized compressible algorithm and the Christopherson one

When performing usual finite difference discretization with mesh size Δx for one dimensional Reynolds equation, equations (13) is detailed at the m^{th} iteration as:

$$p_{k+1}^{m}\left(\left[\frac{\rho(p\ )}{12\mu(p\ )}h^{3}\right]_{k+1/2}^{m-1}+p_{k-1}^{m}\left(\left[\frac{\rho(p\ )}{12\mu(p\ )}h^{3}\right]_{k-1/2}^{m-1}+\frac{u}{2}\Delta x\left[\rho(p)h\right]_{k-1}^{m-1}\right.\right.$$
$$=\frac{u}{2}\Delta x\left[\rho(p)h\right]_{k}^{m}+p_{k}^{m}\left(\left[\frac{\rho(p)}{12\mu(p)}h^{3}\right]_{k-1/2}^{m-1}+\left[\frac{\rho(p\ )}{12\mu(p)}h^{3}\right]_{k+1/2}^{m-1}\right)$$

$[f]^{m}_{k}$ represents the value of expression f at location ($k\Delta x$) at iteration m. As usual in Gauss Seidel procedure , it is not necessary to index the terms with the figure m of the iteration so that this index is not written in the following algorithms.

Algorithm for Implicit linearized method (Gauss Seidel) described in section 3.3 is:

Data: $p_{sat,}\Delta x, \rho_l, \rho_{\inf}, p_{\inf}, \mu(p)$

delta=p_{sat}-p_{inf}

%simplified density pressure law:

$\rho(p)=\rho_{inf}$ if *$p<p_{inf}$* *$\rho(p)=\rho_l (p-p_{inf})/(p_{cav}-p_{inf})+\rho_{inf}$* if *$p_{inf}<p<p_{cav}$* *$\rho(p)=\rho_l$* *if $p>p_{cav}$*

$$
\begin{cases}
loop\ \ for\ iteration\ m \\
\quad \begin{cases}
loop\ \ for\ iteration\ k \\
k=1 \\
A=\left[\dfrac{\rho(p)}{12\mu(p)}h^3\right]_{k-1/2}+\left[\dfrac{\rho(p)}{12\mu(p)}h^3\right]_{k+1/2} \quad B=\dfrac{u}{2}\Delta x[h]_k \\
D=p_{k+1}\left(\left[\dfrac{\rho(p)}{12\mu(p)}h^3\right]_{k+1/2}+p_{k-1}\left(\left[\dfrac{\rho(p)}{12\mu(p)}h^3\right]_{k-1/2}+\dfrac{u}{2}\Delta x[\rho(p)h]_{k-1}\right.\right. \\
prop1=(D+B\ \rho_{\inf})/A; \qquad prop2=(D+B\ \rho_l)/A \\
prop3=[delta\ D+B\ (delta\ \rho_{\inf}-p_{\inf}\ \rho_l)]/(delta\ A-B\rho_l) \\
if\ (prop1\le p\inf)\ p_k=prop1 \\
if\ (prop2\ge psat)\ p_k=prop2 \\
if\ (p\inf\le prop3\le psat)\ p_k=prop3 \\
k\to k+1
\end{cases}
\end{cases}
$$

It can be compared with the usual algorithm for Christopherson method (Gauss-Seidel):

Data: $p_{sat}, \Delta x, \rho_l, \mu(p)$

$\rho(p)=\rho_l$

$$
\begin{cases}
loop\ \ for\ iteration\ m \\
\quad \begin{cases}
loop\ \ for\ iteration\ k \\
k=1 \\
A=\left[\dfrac{\rho(p)}{12\mu(p)}h^3\right]_{k-1/2}+\left[\dfrac{\rho(p)}{12\mu(p)}h^3\right]_{k+1/2} \qquad B=\dfrac{u}{2}\Delta x[h]_k \\
D=p_{k+1}\left(\left[\dfrac{\rho(p)}{12\mu(p)}h^3\right]_{k+1/2}+p^n_{k-1}\left(\left[\dfrac{\rho(p)}{12\mu(p)}h^3\right]_{k-1/2}+\dfrac{u}{2}\Delta x[\rho(p)h]_{k-1}\right.\right. \\
\quad prop2=(D+B\rho_l)/A \\
p_k=\max(p_{sat}, prop2) \\
k \to k+1
\end{cases}
\end{cases}
$$